



Archived at the Flinders Academic Commons:

<http://dspace.flinders.edu.au/dspace/>

‘This is the peer reviewed version of the following article: Ziaei-poor, H., Martelli, S., Pandey, M., & Taylor, M. (2019). Efficacy and efficiency of multivariate linear regression for rapid prediction of femoral strain fields during activity. *Medical Engineering & Physics*, 63, 88–92. <https://doi.org/10.1016/j.medengphy.2018.12.001> ,

which has been published in final form at

<https://doi.org/10.1016/j.medengphy.2018.12.001>

© 2018 IPPEM. Published by Elsevier Ltd. This manuscript version is made available under the CC-BY-NC-ND 4.0 license:<http://creativecommons.org/licenses/by-nc-nd/4.0/>

31 **Abstract**

32 Multivariate Linear Regression-based (MLR) surrogate models were explored to reduce the
33 computational cost of predicting femoral strains during normal activity in comparison with
34 finite element analysis. The musculoskeletal model of one individual, the finite-element
35 model of the right femur, and experimental force and motion data for normal walking, fast
36 walking, stair ascent, stair descent, and rising from a chair were obtained from a previous
37 study. Equivalent Von Mises strain was calculated for 1000 frames uniformly distributed
38 across activities. MLR surrogate models were generated using training sets of 50, 100, 200
39 and 300 samples. The finite-element and MLR analyses were compared using linear
40 regression. The Root Mean Square Error (RMSE) and the 95th percentile of the strain error
41 distribution were used as indicators of average and peak error. The MLR model trained using
42 200 samples (RMSE < 108 $\mu\epsilon$; peak error < 228 $\mu\epsilon$) was used as a reference. The finite-
43 element method required 66 secs per frame on a standard desktop computer. The MLR model
44 required 0.1 sec per frame plus 1848 secs of training time. RMSE ranged from 1.2% to 1.3%
45 while peak error ranged from 2.2% to 3.6% of the maximum micro-strain (5020 $\mu\epsilon$).
46 Performance within an activity was lower during early and late stance, with RMSE of 4.1%
47 and peak error of 8.6% of the maximum computed micro-strain. These results show that
48 MLR surrogate models may be used to rapidly and accurately estimate strain fields in long
49 bones during daily physical activity.

50

51 Keywords: *musculoskeletal; finite-element; surrogate model; human gait*

52

53

54

55 **1. Introduction**

56

57 Quantifying femoral strain distribution is important for studying bone adaptation [1-3],
58 diagnosing individuals most at risk of femoral fracture [4-6], and optimizing the
59 biomechanical behaviour of implantable devices [7, 8]. Over the last few decades, finite-
60 element analysis has been used extensively to quantify the entire femoral strain field [9-11],
61 and there is growing interest in using this method to characterise strain distributions in
62 multiple individuals [12, 13] and across multiple trials and tasks [14]. In addition, there is
63 need to investigate the influence of the musculoskeletal (MS) modelling process on femoral
64 strain predictions, by performing probabilistic analyses to account for uncertainties in the MS
65 model input parameters [14-16] and examining alternative muscle recruitment strategies [17].
66 Unfortunately, the computational cost of performing such analyses can be prohibitive, thus
67 new methods are needed to accurately and rapidly estimate the femoral strain field to enable
68 large-scale studies of 100's to 1000's of simulations to be performed.

69 Surrogate models represent a viable solution in that they can be trained using finite
70 element calculations of femoral strain for a limited number of training sets and then used to
71 rapidly provide femoral strain estimates for an arbitrary frame of motion or an entire activity.
72 A variety of surrogate models have been used by the biomechanics community including
73 Multivariate Linear Regression [18, 19], Bayesian modelling [20], Artificial Neural Networks
74 [18, 21, 22], Random Forest [23] and Kriging [24-26], either for linear problems, (e.g.,
75 assessment of femoral neck fracture during a single load case [18]) or for non-linear problems
76 (e.g., modelling the contact between bone and implant [19]). Most studies predict a single
77 scalar outcome, such as joint moments and muscle forces [27]; contact forces and contact
78 pressure [21, 25, 26, 28-30]; femoral neck strain and fracture load [18]; implant micro-
79 movement and stress shielding [20, 31]. Multivariate Linear Regression has been used for

80 predicting femoral neck strain [32], fracture load [18] and the micro-movement at the bone-
81 implant interface [19]. However, the error and computational advantage of MLR over finite-
82 element models remains unclear for the calculation of strain over the femoral volume and
83 across normal activities of daily living.

84 The aim of this work was to explore the use of MLR for predicting femoral strain fields
85 for a range of activities of daily living. Muscle forces, joint reaction forces and femoral strain
86 were calculated for a single individual performing five tasks using a previously developed
87 musculoskeletal and finite-element model [16]. A MLR surrogate model was trained using
88 femoral strain, muscle forces, and joint reaction forces for a limited number of randomly
89 selected frames of motion and then used to estimate femoral strain for multiple motor tasks.
90 Model performance was assessed by comparing MLR estimates of the femoral strain field to
91 corresponding results obtained from finite-element calculations.

92

93 **2. Materials and Methods**

94 ***2.1 Data***

95 A full-body musculoskeletal model, finite-element model of the femur of the dominant
96 leg, marker trajectories, and ground reaction forces for a single healthy participant (female,
97 68-year-old, 53 kg weight, 157 cm height) were obtained from a previous study [16]. All
98 experimental and computational methods are described in detail by Martelli et al. (2015) and
99 Dorn et al. (2012), respectively. Briefly, marker trajectories and ground reaction forces were
100 recorded for five trials of each of the following five tasks: walking at the self-selected speed
101 (normal walking), fast walking, stair ascent, stair descent, and rising from and sitting down
102 on a chair (chair rise). Trials with incomplete marker trajectories were discarded, resulting in
103 five trials each for normal walking, fast walking and stair descent; four trials for stair ascent;
104 and one trial for chair rise. A participant-specific musculoskeletal model was created by

105 scaling the generic model described by Dorn et al. (2012) using the segment lengths and body
106 mass measured during a static trial.

107 The marker trajectories were labelled using a VICON motion capture system (Vicon,
108 Oxford, UK), saved as c3d files, and then converted into OpenSim format using MOtoNMS
109 [34]. Joint angles, muscle forces, and joint reaction forces were calculated using,
110 respectively, inverse kinematics, static optimization and joint reaction analysis tools available
111 in OpenSim [35]. The finite-element model of the right femur was a locally-isotropic, linear-
112 elastic model whose geometry and element-by-element material properties were extracted
113 from calibrated computed-tomography images following a well-established procedure [36].
114 The finite-element model was loaded by applying muscle forces and the hip joint reaction
115 force for 50 frames uniformly distributed over each activity. The FE model was kinematically
116 constrained distally (Figure 1). The musculoskeletal and finite-element models were coupled
117 using custom software [16]. The equivalent von Mises strain was calculated at each element
118 centroid for a total of 1000 frames (20 trials, 50 frames per trial) as a compact indicator of
119 both compressive and tensile strain states.

120 ***2.2 Multi-variate linear regression surrogate model***

121 A Latin Hypercube (LH) sampling method was used to create the training set, which
122 comprised of muscle forces, joint reaction forces and femoral strains for randomly selected
123 frames of motion (Figure 1). The process was repeated to generate four training sets
124 consisting of 50, 100, 200 and 300 frames, respectively. Training sets of similar size have
125 been used to develop surrogate models in previous studies [19, 24]. The surrogate model,
126 relating the applied forces to the equivalent von Mises strain, was developed by fitting a
127 MLR model for each element. The model took the form:

$$\varepsilon^{j,k} = \sum_{i=0}^{25} (c_i \times f_i^k); f_1^k, \dots, f_{25}^k$$

128 where $\varepsilon^{j,k}$ is the equivalent von Mises strain at element j for frame k , and c_i is the coefficient
129 for the force i at frame k . The total number of forces applied to the finite-element model was
130 25, which included all the muscle forces in the musculoskeletal model acting on the femur
131 and the hip reaction force. The strain field for all 1000 frames of motion was calculated using
132 the calculated coefficients c_i in the MLR model and corresponding muscle and joint reaction
133 forces. Performance of the MLR surrogate models was assessed by calculating the coefficient
134 of determination (R^2) and the slope of the linear regression between the strains predicted by
135 the surrogate and finite-element models. CPU times needed to complete the finite-element
136 analysis, train the MLR models, and calculate femoral strain using the MLR models were
137 compared on a standard desktop computer (8 CPUs Intel® Core(TM)® 3.4 GHz processor, 32
138 GB RAM). Strain error was calculated using the finite-element strain as a reference and
139 evaluated using the Root Mean Square Error (RMSE) as well as the 95th percentile of the
140 strain error distribution as an indicator of peak error. These parameters were analysed frame-
141 by-frame within each trial (i.e. $RMSE_{Frame}; R_{Frame}^2$) by amalgamating all frames for each
142 trial (i.e. $RMSE_{Trial}; R_{Trial}^2$) and for each activity (i.e. $RMSE_A; R_A^2$).

143

144 **3. Results**

145 The trial-by-trial comparison showed that the coefficient of determination and slope
146 were close to unity for the training datasets greater than 50 ($R_{Trial}^2 = 0.84 - 0.94$;
147 $slope_{Trial} = 0.97 - 0.99$). The prediction error of the surrogate model was a function of the
148 size of the training set. Increasing the size of the training set from 100 to 200 frames reduced
149 the average RMSE across trials from 132 $\mu\varepsilon$ to 108 $\mu\varepsilon$, while a relatively small decrease in

150 RMSE to $107 \mu\epsilon$ was obtained by increasing the training set size to 300 samples (Table 1).
151 Based on these observations, the remainder of the results are presented only for the MLR
152 model trained using 200 samples.

153 CPU time for predicting the full femoral strain for all 1,000 frames was 66,000 secs using
154 the finite-element model alone (i.e., 55 minutes were necessary for predicting femoral strain
155 for an entire activity of 50 frames). Training the MLR model required 13,200 secs for
156 completing the 200 finite-element simulations in the training set, 528 secs for training and
157 100 secs for predicting all 1,000 frames, which corresponds to 5 secs for predicting femoral
158 strain for an entire activity (50 frames). The MLR-based surrogate model was faster than
159 finite-element analysis for solving 209 frames or more (Figure 2).

160 Similar performance of the MLR model was observed for all activities. The median $RMSE_A$
161 varied between $80 \mu\epsilon$ for normal walking and $124 \mu\epsilon$ for chair rise. Peak $RMSE_A$ varied from
162 $163 \mu\epsilon$ for stair ascent to $389 \mu\epsilon$ for chair rise (Figure 3).

163 The performance of the MLR model is presented for a selected trial of normal walking as
164 an exemplar activity (Figures 4 and 5). Close visual agreement was observed between the
165 strain distributions estimated by the surrogate model and those predicted by the FE model
166 (Figure 4). The average RMSE and peak error were 78 and $181 \mu\epsilon$, respectively, across
167 different frames. RMSE reached $207 \mu\epsilon$ during early stance and $140 \mu\epsilon$ during late stance
168 while the corresponding peak errors reached $433 \mu\epsilon$ and $391 \mu\epsilon$, respectively, for early and
169 late stance (Figure 5). The peak error was 8.6% of peak equivalent strain in the diaphysis,
170 ranging from approximately 2920 to $5020 \mu\epsilon$ during the stance phase of gait. The average
171 coefficient of determination and slope were 0.97 and 0.99, respectively.

172

173 **4. Discussion**

174 Finite element analysis has been used extensively in orthopaedic biomechanics
175 research [37], but there are a number of barriers involved in the translation of FE modelling
176 to the clinic. One problem is that predicting the full femoral strain for multiple tasks using a
177 coupled FE-musculoskeletal modelling approach is computationally expensive. The current
178 study represents a first step in overcoming this barrier, by demonstrating that reliable
179 estimates of strain distributions may be obtained rapidly. Surrogate models offer a potentially
180 powerful alternative as they provide predictions of bone strains in seconds rather than hours.
181 The present study evaluated the performance of a multivariate linear regression surrogate
182 model in approximating the full strain field of an intact femur during five different activities
183 of daily living.

184 We found that reliable predictions of femoral strain could be obtained across all five
185 activities by training the surrogate model using 200 samples. The surrogate model closely
186 reproduced the FE results at a low computational cost, with typical solution times of 5 secs
187 per activity (50 frames) compared to 55 minutes needed for a finite-element analysis.

188 The predicted strains from the MLR model were in close agreement with those
189 obtained using the finite-element model. The peak error in the MLR model was 8.6% of the
190 peak equivalent strain (5020 $\mu\epsilon$), which is comparable to the error (i.e., 4.2 – 8.3% of peak
191 strain on average) caused by material properties and geometry errors committed while
192 generating the finite-element models from calibrated computed-tomography images [38].
193 Furthermore, the average RMSE was 78 $\mu\epsilon$, which is consistent with the average error (113
194 $\mu\epsilon$) obtained when finite-element models are used to predict experimentally measured
195 cortical strains [38]. Therefore, MLR models represent valid surrogates of finite-element
196 calculations of femoral strain during activity. The training sample size was similar to that
197 reported in previous surrogate modelling studies in biomechanics: Fitzpatrick et al. (2014)
198 required 100 – 200 samples for a MLR-based surrogate model; Taylor et al. (2017) needed

199 200 – 500 samples to train an artificial neural network; and Lin et al. (2009) required 300
200 samples to develop a kriging-based surrogate model. This supports the validity of the MLR
201 model developed in the present study.

202 The current study is not without limitations. Firstly, Latin Hypercube sampling was
203 used to generate the training datasets, but generating more uniformly distributed samples
204 using other potential techniques may improve model accuracy. Secondly, the performance of
205 the surrogate model was lowest during early stance where the coefficient of determination
206 was only 0.53. This error is likely caused by the non-linear behaviour of the model, arising,
207 for example, from the displacement of the hip centre of pressure during motion. Different
208 surrogate methods (e.g. MARS, Gaussian Process and Artificial Neural Networks) may
209 further improve model performance. Thirdly, the prediction time of the MLR model (0.1 sec
210 per frame) was much faster than that of the finite-element model, although the MLR required
211 200 finite-element simulations for generating the training set and 528 secs for training the
212 model. Thus, the MRL model is computationally advantageous relative to the finite-element
213 model only when 209 frames of motion or more are to be analysed (Figure 2). Fourth, only
214 normal activities were included in the reference study [16] to limit the risk of injury for the
215 participants while executing demanding (e.g., sprinting) or para-physiological (e.g., falling)
216 activities. Therefore, the validity of the present conclusion is limited to normal locomotion.
217 Fifth, the MLR model was developed for a single healthy individual possibly limiting the
218 generality of the present conclusions. However, the strain range predicted by the model (0 –
219 5020 $\mu\epsilon$) spans a large portion of physiologically admissible strains [39] and the loading
220 conditions did span a broad range of normal activities, providing confidence on the
221 performance of the MLR model over a relevant range of femoral strain and boundary
222 conditions of the femur.

223

224 **5. Conclusions**

225 A Multivariate Linear Regression model was successfully developed for a single individual
226 and used to rapidly predict the full femoral strain field for a range of activities of daily living.
227 The MLR model was able to predict the femoral strain field for each studied activity within
228 an error comparable to the intrinsic error in finite-element models based on clinical CT
229 images and was computationally advantageous when 209 loading cases or more were
230 analysed. Hence, MLR enables large statistical studies of femoral strain during activity.

231

232

233 **Competing interests:** There are no conflicts of interest associated with the work performed
234 in this study.

235 **Funding:** This work was supported by the Australian Government Research Training
236 Program Scholarship (AGRTPS); and the Australian Research Council [DP180103146].

237 **Ethical approval:** Not required

238

239

240

241

242

243

244

245

246

247 **6. References**

248 [1] Geraldles DM, Modenese L, Phillips ATM. Consideration of multiple load cases is critical
249 in modelling orthotropic bone adaptation in the femur. *Biomech Model Mechanobiol.*
250 2016;15:1029-42.

251 [2] Adams DJ, Spirt AA, Brown TD, Fritton SP, Rubin CT, Brand RA. Testing the daily
252 stress stimulus theory of bone adaptation with natural and experimentally controlled strain
253 histories. *J Biomech.* 1997;30:671-8.

254 [3] Duda GN, Heller M, Albinger J, Schulz O, Schneider E, Claes L. Influence of muscle
255 forces on femoral strain distribution. *J Biomech.* 1998;31:841-6.

256 [4] Bessho M, Ohnishi I, Matsumoto T, Ohashi S, Matsuyama J, Tobita K, et al. Prediction of
257 proximal femur strength using a CT-based nonlinear finite element method: Differences in
258 predicted fracture load and site with changing load and boundary conditions. *Bone.*
259 2009;45:226-31.

260 [5] Bessho M, Ohnishi I, Matsuyama J, Matsumoto T, Imai K, Nakamura K. Prediction of
261 strength and strain of the proximal femur by a CT-based finite element method. *J Biomech.*
262 2007;40:1745-53.

263 [6] Lotz JC, Cheal EJ, Hayes WC. Fracture prediction for the proximal femur using finite
264 element models: Part II--Nonlinear analysis. *J Biomech Eng.* 1991;113:361-5.

265 [7] Helwig P, Faust G, Hindenlang U, Hirschmuller A, Konstantinidis L, Bahrs C, et al.
266 Finite element analysis of four different implants inserted in different positions to stabilize an
267 idealized trochanteric femoral fracture. *Injury.* 2009;40:288-95.

268 [8] Chanda S, Dickinson A, Gupta S, Browne M. Full-field in vitro measurements and in
269 silico predictions of strain shielding in the implanted femur after total hip arthroplasty. *Proc*
270 *Inst Mech Eng H.* 2015;229:549-59.

271 [9] Martelli S, Pivonka P, Ebeling PR. Femoral shaft strains during daily activities:
272 Implications for atypical femoral fractures. *Clin Biomech.* 2014;29:869-76.

273 [10] Martelli S. Femoral neck strain during maximal contraction of Isolated hip-spanning
274 muscle groups. *Comput Math Methods Med.* 2017;Article ID 2873789.
275 <https://doi.org/10.1155/2017/2873789>.

276 [11] Al-Dirini RMA, Huff D, Zhang J, Besier T, Clement JG, Taylor M. Influence of collars
277 on the primary stability of cementless femoral stems: A finite element study using a diverse
278 patient cohort. *J Orthop Res.* 2018;36:1185-95.

279 [12] Bryan R, Nair PB, Taylor M. Use of a statistical model of the whole femur in a large
280 scale, multi-model study of femoral neck fracture risk. *J Biomech.* 2009;42:2171-6.

- 281 [13] Zhang J, Besier TF. Accuracy of femur reconstruction from sparse geometric data using
282 a statistical shape model. *Comput Methods Biomech Biomed Engin.* 2016;20:566-76.
- 283 [14] Martelli S, Valente G, Viceconti M, Taddei F. Sensitivity of a subject-specific
284 musculoskeletal model to the uncertainties on the joint axes location. *Comput Methods*
285 *Biomech Biomed Engin.* 2015;18:1555-63.
- 286 [15] Ackland DC, Lin YC, Pandy MG. Sensitivity of model predictions of muscle function to
287 changes in moment arms and muscle-tendon properties: a Monte-Carlo analysis. *J Biomech.*
288 2012;45:1463-71.
- 289 [16] Martelli S, Kersh ME, Pandy MG. Sensitivity of femoral strain calculations to
290 anatomical scaling errors in musculoskeletal models of movement. *J Biomech.* 2015;48:3606-
291 15.
- 292 [17] Martelli S, Calvetti D, Somersalo E, Viceconti M. Stochastic modelling of muscle
293 recruitment during activity. *Interface Focus.* 2015;5:20140094. doi: 10.1098/rsfs.2014.0094.
- 294 [18] Taylor M, Perilli E, Martelli S. Development of a surrogate model based on patient
295 weight, bone mass and geometry to predict femoral neck strains and fracture loads. *J*
296 *Biomech.* 2017;55:121-7.
- 297 [19] Fitzpatrick CK, Hemelaar P, Taylor M. Computationally efficient prediction of bone-
298 implant interface micromotion of a cementless tibial tray during gait. *J Biomech.*
299 2014;47:1718-26.
- 300 [20] Bah MT, Nair PB, Taylor M, Browne M. Efficient computational method for assessing
301 the effects of implant positioning in cementless total hip replacements. *J Biomech.*
302 2011;44:1417-22.
- 303 [21] Eskinazi I, Fregly BJ. Surrogate modeling of deformable joint contact using artificial
304 neural networks. *Med Eng Phys.* 2015;37:885-91.
- 305 [22] Liang L, Liu M, Martin C, Sun W. A deep learning approach to estimate stress
306 distribution: a fast and accurate surrogate of finite-element analysis. *J R Soc Interface.*
307 2018;15:20170844. doi: 10.1098/rsif.2017.0844.
- 308 [23] Donaldson FE, Nyman Jr E, Coburn JC. Prediction of contact mechanics in metal-on-
309 metal Total Hip Replacement for parametrically comprehensive designs and loads. *J*
310 *Biomech.* 2015;48:1828-35.
- 311 [24] O'Rourke D, Martelli S, Bottema M, Taylor M. A computational efficient method to
312 assess the sensitivity of finite-element models: An illustration with the hemipelvis. *J Biomech*
313 *Eng.* 2016;138. doi: 10.1115/1.4034831.
- 314 [25] Walter JP, Pandy MG. Dynamic simulation of knee-joint loading during gait using
315 force-feedback control and surrogate contact modelling. *Med Eng Phys.* 2017;48:196-205.
- 316 [26] Lin YC, Haftka RT, Queipo NV, Fregly BJ. Two-dimensional surrogate contact
317 modeling for computationally efficient dynamic simulation of total knee replacements. *J*
318 *Biomech Eng.* 2009;131:041010. doi: 10.1115/1.3005152.

- 319 [27] Favre J, Hayoz M, Erhart-Hledik JC, Andriacchi TP. A neural network model to predict
320 knee adduction moment during walking based on ground reaction force and anthropometric
321 measurements. *J Biomech.* 2012;45:692-8.
- 322
- 323 [28] Pizzolato C, Reggiani M, Saxby DJ, Ceseracciu E, Modenese L, Lloyd DG. Biofeedback
324 for gait retraining based on real-time estimation of tibiofemoral joint contact forces. *IEEE*
325 *Trans Neural Syst Rehabil Eng.* 2017;25:1612-21.
- 326 [29] Lin YC, Haftka RT, Queipo NV, Fregly BJ. Surrogate articular contact models for
327 computationally efficient multibody dynamic simulations. *Med Eng Phys.* 2010;32:584-94.
- 328 [30] Halloran JP, Erdemir A, van den Bogert AJ. Adaptive surrogate modeling for efficient
329 coupling of musculoskeletal control and tissue deformation models. *J Biomech Eng.*
330 2009;131: 011014. doi: 10.1115/1.3005333.
- 331 [31] Cilla M, Borgiani E, Martínez J, Duda GN, Checa S. Machine learning techniques for
332 the optimization of joint replacements: Application to a short-stem hip implant. *PLoS One.*
333 2017;12:e0183755. doi: <https://doi.org/10.1371/journal.pone.0183755>.
- 334 [32] Kersh ME, Martelli S, Zebaze R, Seeman E, Pandy MG. Mechanical loading of the
335 femoral neck in human locomotion. *J Bone Miner Res.* 2018. 33:1999-2006.
336 doi: 10.1002/jbmr.3529.
- 337
- 338 [33] Dorn TW, Schache AG, Pandy MG. Muscular strategy shift in human running:
339 dependence of running speed on hip and ankle muscle performance. *J Exp Biol.*
340 2012;215:1944-56.
- 341 [34] Mantoan A, Pizzolato C, Sartori M, Sawacha Z, Cobelli C, Reggiani M. MOtoNMS: A
342 MATLAB toolbox to process motion data for neuromusculoskeletal modeling and
343 simulation. *Source Code Biol Med.* 2015;10:1-14.
- 344 [35] Delp SL, Anderson FC, Arnold AS, Loan P, Habib A, John CT, et al. OpenSim: open-
345 source software to create and analyze dynamic simulations of movement. *IEEE Trans*
346 *Biomed Eng.* 2007;54:1940-50.
- 347 [36] Taddei F, Cristofolini L, Martelli S, Gill HS, Viceconti M. Subject-specific finite
348 element models of long bones: An in vitro evaluation of the overall accuracy. *J Biomech.*
349 2006;39:2457-67.
- 350 [37] Taylor M, Prendergast PJ. Four decades of finite element analysis of orthopaedic
351 devices: Where are we now and what are the opportunities? *J Biomech.* 2015;48:767-78.
- 352 [38] Taddei F, Martelli S, Reggiani B, Cristofolini L, Viceconti M. Finite-element modeling
353 of bones from CT data: sensitivity to geometry and material uncertainties. *IEEE Trans*
354 *Biomed Eng.* 2006;53:2194-200.
- 355 [39] Bayraktar HH, Morgan EF, Niebur GL, Morris GE, Wong EK, Keaveny TM.
356 Comparison of the elastic and yield properties of human femoral trabecular and cortical bone
357 tissue. *J Biomech.* 2004;37:27-35.

Figure Captions

Figure 1. Flowchart illustrating the linear-based surrogate modelling approach used in the present study.

Figure 2. CPU time required by the finite-element model and MLR model plotted against the number of frames.

Figure 3. Box plots used to quantify the accuracy of model-predicted strains obtained from MLR surrogate modelling. The black box represents the range of the error between the 25th and 75th percentiles while the red horizontal dashed line represents the median error. The black dashed line represents the 95th percentile of $RMSE_A$ for each activity.

Figure 4. Contour plots showing the calculated femoral strain fields for normal walking obtained by applying finite element modelling (FEM) and MLR surrogate modelling. Results are shown at 25% intervals of the stance phase. 0% and 100% indicate the stance phase.

Figure 5. Evaluating the performance of the MLR surrogate model for normal walking: (a) pattern of the hip joint reaction force; (b) coefficient of determination (R_{Frame}^2); (c) peak error and root mean square error ($RMSE_{Frame}$) at each frame. BW in part (a) refers to body weight; the red dots shown in part (b) represent the frames used to train the surrogate model

Figure 1

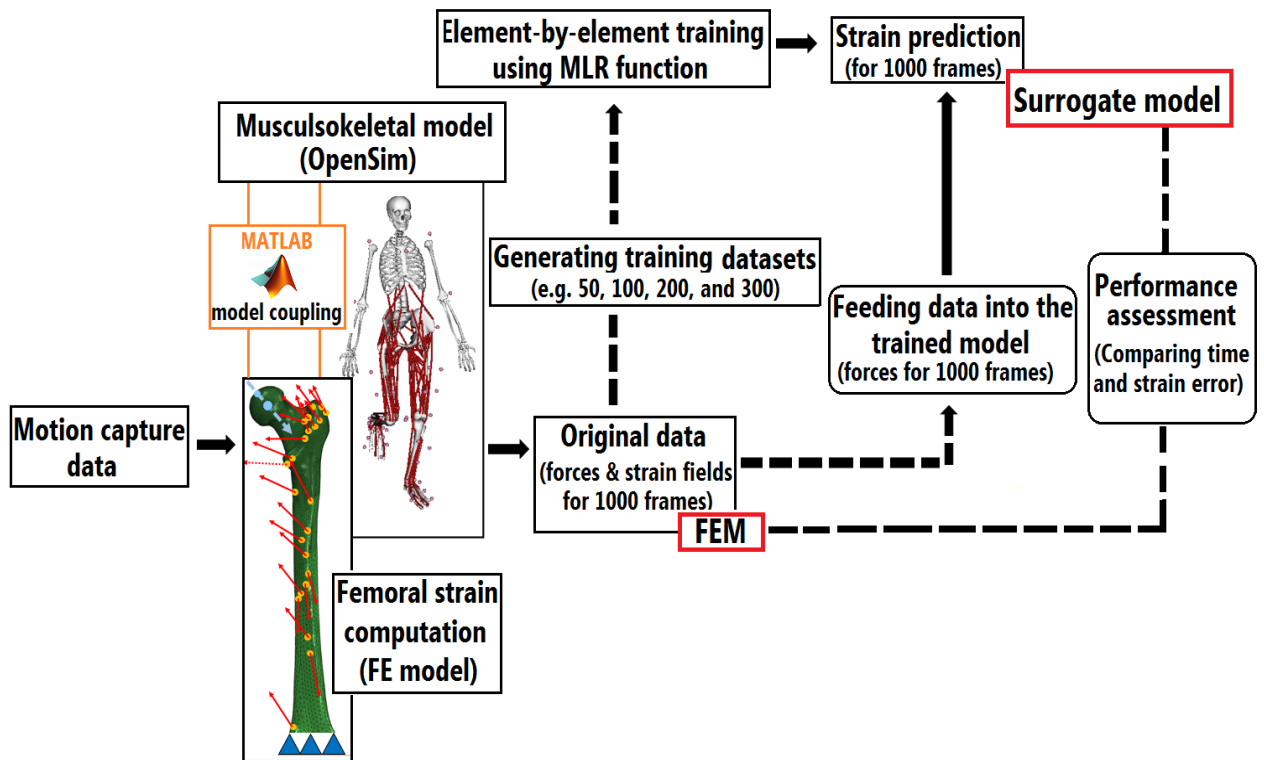


Figure 2

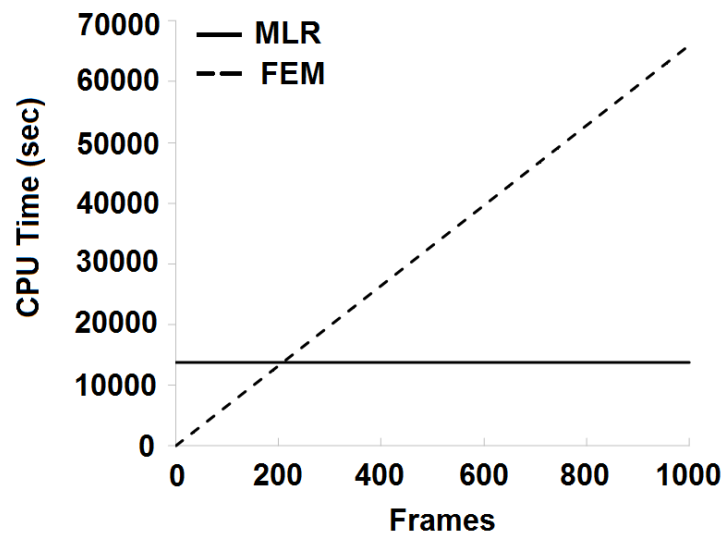


Figure 3

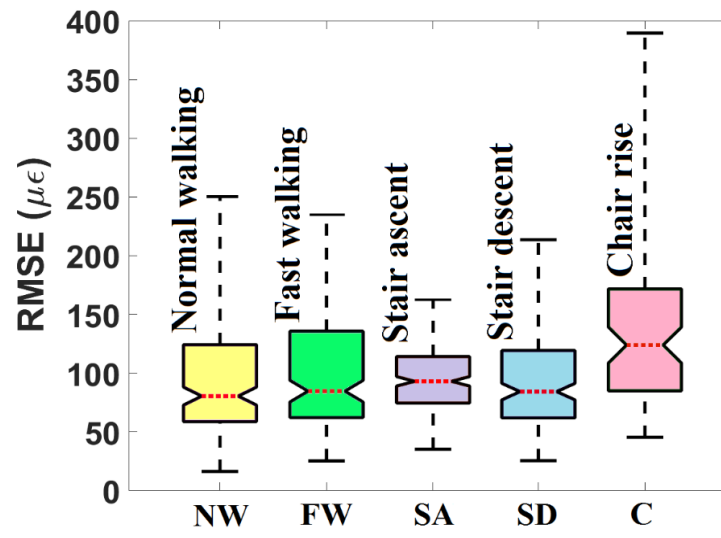


Figure 4

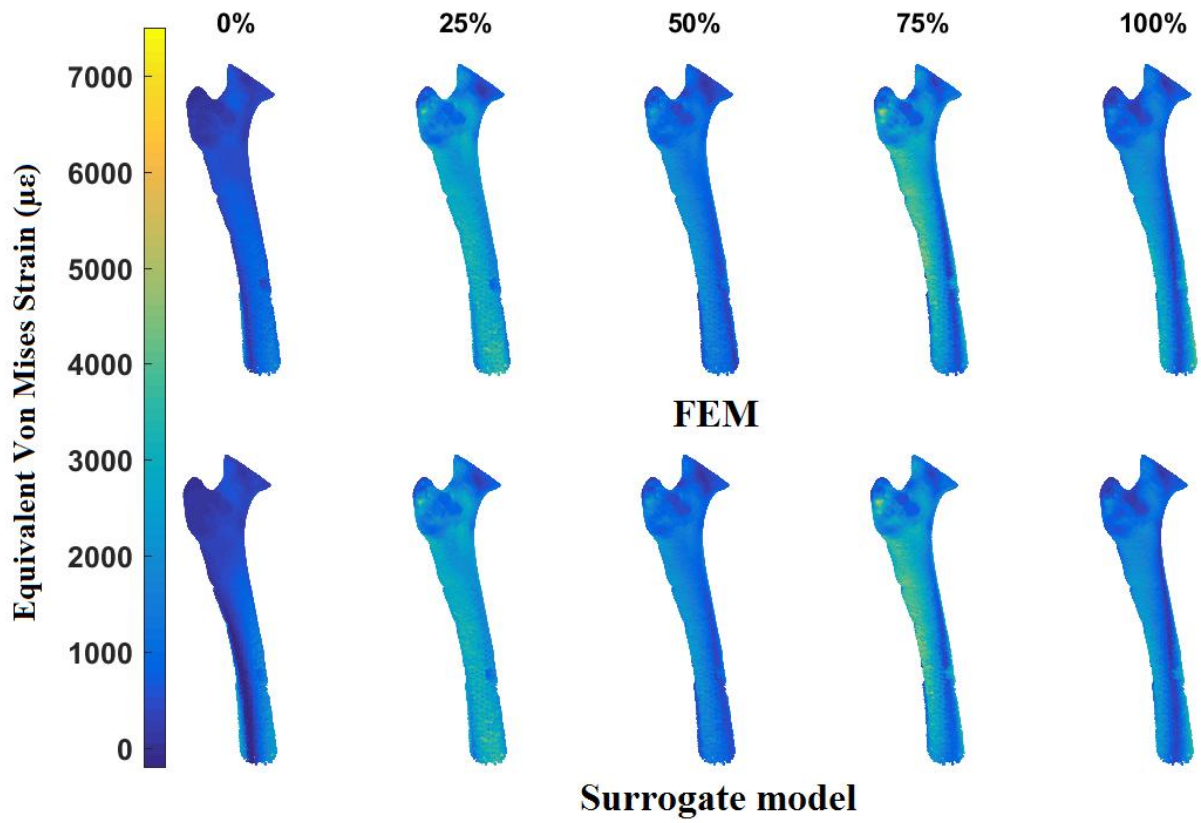
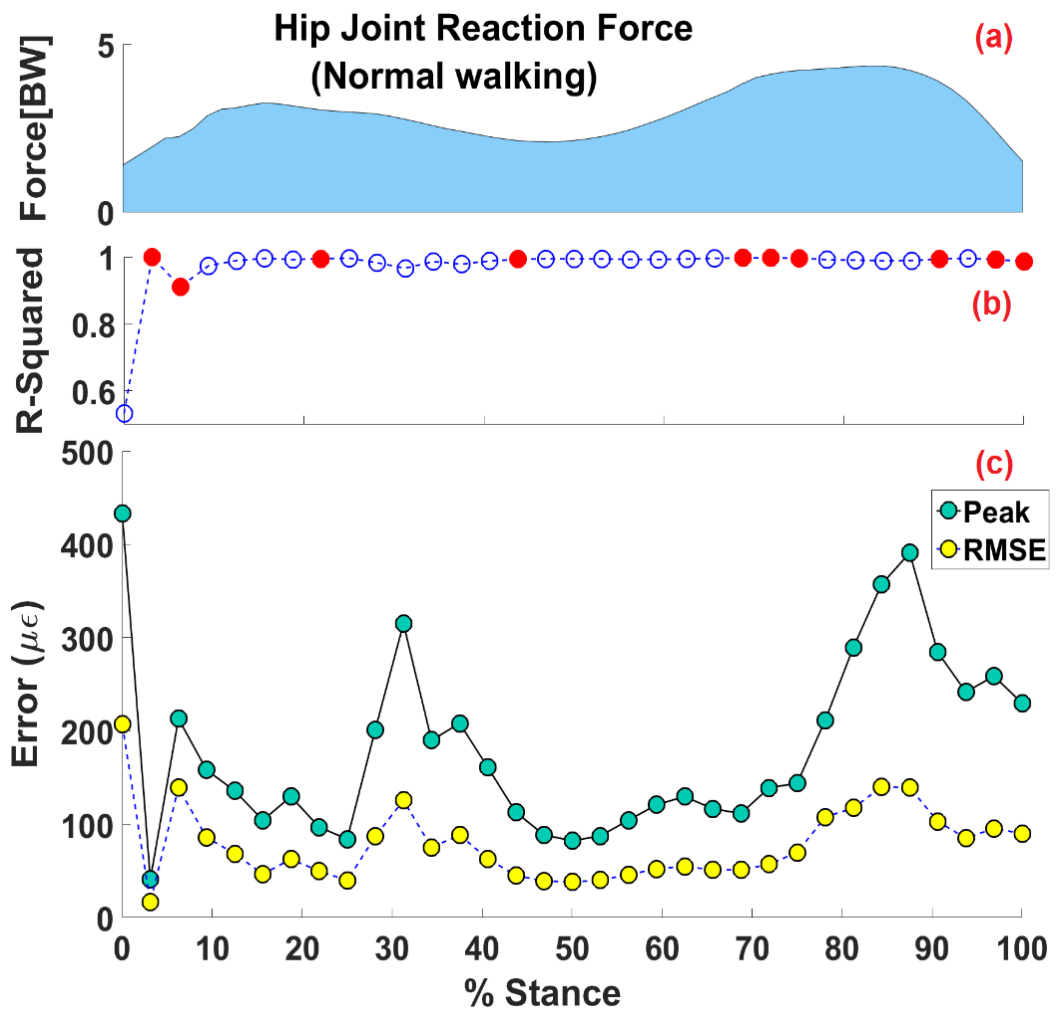


Figure 5



Tables.

Table 1. Effect of the size of training datasets on the accuracy of model-predicted femoral strains. Model accuracy was evaluated by computing the mean and peak error and the mean of coefficient of determination. These reported errors are based on pooled data.

Training Datasets	Mean RMSE ($\mu\epsilon$)	Peak RMSE ($\mu\epsilon$)	Mean R^2	Training Time (min)
50	227	408484	0.84	8.5
100	132	326	0.92	8.7
200	108	228	0.94	8.8
300	107	201	0.94	8.9